16th World Conference on Earthquake, 16WCEE 2017
Santiago Chile, January 9th to 13th 2017
Paper N° 1006
Registration Code: S-XXXXXXXX

UNUSUAL FINDINGS AFTER THE 2015 NEPAL GORKHA M 7.8 EARTHQUAKE FROM ENGINEERING AND GEOLOGICAL POINTS OF VIEW

P. Carydis[(1)], E. Lekkas[(2)], I. Taflampas[(3)], E. Skourtsos[(4)], S. Markantonis[(5)], S. Mavroulis[(6)]

[(1)] *Professor of Earthquake Engineering, Professor Emeritus of the National Technical University of Athens, Greece, Member of the European Academy of Sciences and Arts, Panagouli 5a str., Kifissia, Greece, e-mail: pkary@tee.gr (corresponding author)*
[(2)] *Professor of Dynamic Tectonic Applied Geology, Department of Dynamic, Tectonic and Applied Geology, Faculty of Geology and Geoenvironment, School of Sciences, National and Kapodistrian University of Athens, Greece, e-mail: elekkas@geol.uoa.gr*
[(3)] *Civil Engineer Phd, Laboratory Teaching Staff, Laboratory of Earthquake Engineering National Technical University of Athens, Greece, e-mail: taflan@central.ntua.gr*
[(4)] *Geologist Phd, Laboratory Teaching Staff, Department of Dynamic, Tectonic and Applied Geology, Faculty of Geology and Geoenvironment, School of Sciences, National and Kapodistrian University of Athens, Greece, e-mail: eskourt@geol.uoa.gr*
[(5)] *Civil Engineer MSc, e-mail: markantona@yahoo.gr*
[(6)] *Geologist MSc, PhD Candidate, Department of Dynamic Tectonic Applied Geology, Faculty of Geology and Geoenvironment, School of Sciences, National and Kapodistrian University of Athens, Greece, e-mail: smavroulis@geol.uoa.gr*

Abstract

Despite the large magnitude of the earthquake and the shallow depth of its focus, not a consistent surface faulting was observed, except one site at the city of Kathmandu. The city is about 76 km to the SE-E of the epicenter of the main shock. This distance, in general, might be considered as rather long, but the observed faulting could be justified due to the very small inclination (dipping angle about 100) of the faulting plane towards north, in combination with the depth and the location of the focus.

The incurred structural damage was extended over a rather large area along the main axis of the country from about 120 km (E-W) to 50 km (N-S). The intensity of the damage was strongly varying all over this vast region, even among adjacent plots, and closely lying structures. On the other hand, it was not observed the well known diminuation or the differentiation of damage as a basic function of epicentral distance up to around 80 km. Even more, the field observations of the response of structures led to a general conclusion that either we had very small no damage, or collapse/heavy damage. Statistically speaking, not intermediate level of damage was observed.

For most of the buildings with fired clay brick masonry and wooden roofs and floors, the observed damage started from the roof and the top floors. This type of structural response implies that the structures have been excited dominantly along the vertical direction, in addition to the fact that they have been collapsed symmetrically around a vertical axis and/or inside their plan. In some cases intermediate floors have been squeezed. In almost all partially collapsed buildings no window glass panels were broken in the uncollapsed part of them. These phenomena are tried to be explained by considering not only the structural characteristics and deficiencies, but also the convolution of different types of emerging seismic waves. The basic characteristics of the ground motion were estimated by an appropriate consideration of each building structure as a kind of a 3-D seismoscope. Its frozen final response is recorded and the causing ground excitation is inferred by applying basic principles of structural mechanics. This methodology may be applied where strong motion records are not available, or are not representative, as the present case is.

Although forward directivity phenomena occurred towards Kathmandu (the rupture was directed towards Kathmandu producing velocity pulses with period larger than 4 sec), they had no effect on structures of the area as proved from the observations of the structural response, a fact that it is tried to be explained. The arguments are supported by the least possible number of characteristic pictures and drawings.

Keywords: Nepal 2015 earthquake; geoscientific findings; vertical earthquake component; forward directivity

1. INTRODUCTION

A violent earthquake of magnitude 7.8 hit Nepal on Saturday April 25th, 2015 at 06:11 UTC (11:56 local time) (Fig. 1a). The shake has been felt all over Nepal, India, Tibet and Bangladesh and caused major damage in Kathmandu and in surrounding cities including a number of centuries-old temples. The death toll exceeds 8,000 victims. The earthquake also triggered avalanches on Mount Everest, which killed at least 17 people at the base camp.

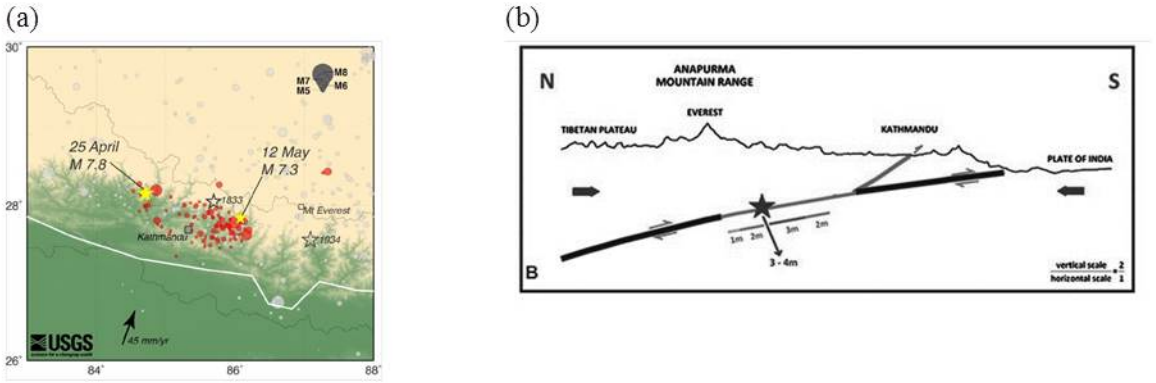

Fig. 1 – (a) Main events and aftershock locations of central Nepal earthquake sequence (USGS, 2015). (b) Sketch showing the proposed model of the fault geometry ruptured during the central Nepal earthquake. The star indicates the hypocenter of the earthquake. Thinner line indicates the ruptured segment of the MHT, while the thicker line the segments that did not activate. The rupture was propagated southwards and eastwards along the MHT and then upwards along a thrust fault that is linked to the MHT. The surficial trace of that fault was observed at the SE suburbs of Kathmandu.

The study team moved to Nepal immediately after the earthquake and visited earthquake stricken sites that were accessible by car, for five days, over a region covering around 60 km to the north-west and around 40 km to the south-east of Kathmandu city. Due to rock falls and landslides it stood impossible to visit the areas around Gorkha.

In the present brief communication are exposed the most interesting observations and is presented an effort to explain the incurred damage. A commentary on societal aspects, on disaster management and on the involvement of the international community is presented, based on the on-site experience of members of the study team during the critical period of five days following the disaster.

The region belongs to the Himalaya Arc, which has suffered a lot of times from very large earthquakes with a moment magnitude of 7.5 or more [1, 2, 3]. The Himalaya orogen is the result of the collision of India and Eurasia that started during latest Paleocene to early Eocene time and the subsequent northward subduction of India [4, 5]. Major Cenozoic normal or thrust faults with a general dip direction towards the north are observed in the Himalaya thrust belt: the Main Frontal Thrust (MFT), the Main Boundary Thrust (MBT), the Main Central Thrust (MCT) and the South Tibetan Detachment System (STDS) [6 and references therein]. All the thrust structures can be observed throughout the mountain chain and it is believed that are linked to a large-scale detachment, the Main Himalayan Thrust (MHT).

2. SEISMOLOGICAL DATA AND DEFORMED ZONES

The earthquake epicenter of the April 25th event was located near the village of Barpak in Gorkha district, which was completely destroyed by the earthquake. USGS assigned the moment magnitude as 7.8 and the event was located at 28.147°N and 84.708°E. The focal depth of the earthquake was only 11-15 km; the activated thrust fault had a WNW-ESE strike with 7^{o}-10^{o} dip towards the north [7]. Seismological data and crustal-scale

geological section, suggest that the earthquake has ruptured a segment of the Main Himalayan Thrust (MHT). The rupture started at the epicenter and propagated eastward for about 130 km, rupturing the area directly located under the Kathmandu basin (Fig. 1b).

To the southeastern suburbs of Kathmandu city, we observed a wide ground deformation zone associated with thrust faulting and mainly the formation of monocline-like escarpments with heights ranged from 0.5m to 1.8m (Fig. 2). Although the deformation was intense at the escarpment, there was noticeable deformation nearby, especially in the hanging wall of the thrust. Different kind of smaller structures such tension cracks and small-amplitude folds were also observed (Fig. 2a-c).

Fig. 2 – (a) View of a spectacular stretch of the central Nepal highly disrupted zone along the northern side of the Araniko Highway, Kathmandu city. The ground was deformed into a monoclinal escarpment with 1.6m of relief. Tension cracks were formed at the crest of the zone. (b) Another view of a monoclonal escarpment in area of tilted bricks along the northern pavement of the Araniko Highway. The ground on the right (NNW) lifted up about 1.3 m relative to the ground on the left (SSE). The crest of the escarpment was broken and discontinuous. Originally flat–lying pavement bricks and the cement slab were tilted near the crest of the escarpment. (c) The concrete yard was broken into polygonal pieces due to ground deformation, which were lifted upward due to N-S compression. Note that the house is unaffected. (d), (e) Many multi storied buildings were tilted without structural damage.

The highly disrupted zone runs diagonally to the Araniko Highway in Gatthaghar, SE of the National Airport, with an average ENE-WSW strike and ranges 200m in width and 1,000m in length. The ground on the north lifted up 1.0-1.8m relative to that on the south forming low monoclonal escarpments (Fig. 2a-b). The deformation zone in the asphalt road presents tensional cracks with a width of 15-60cm with parallel or an en-echelon arrangement and a vertical throw of 20-40 cm.

Further away from the Highway, many buildings throughout the deformation zone were tilted and thereby distorted slightly as solid bodies. However, it is very interesting that structural damage due to direct earthquake effect was not observed in them (Fig. 2d-e). Nevertheless, the ground deformation along the highly disrupted zone caused the damage or even the collapse of small constructions such as walls and pavements in the house yards leaving unaffected the buildings (Fig. 2c).

The above mentioned ground cracks are in agreement with preliminary models of co-seismic slip which suggest that the largest amount of slip on the fault was located just below the city of Kathmandu.

3. COMMENTARY ON THE SEISMIC RESPONSE OF STRUCTURES

The scope of this section is mainly to discuss the response of the various structures and secondarily to infer some basic characteristics of the respective ground motion. The latter one can be determined from a detailed observation of the seismic response of a structure, considering it as a 3D seismoscope the final response of which is frozen.

It must be emphasized that the response of the various types of structures mentioned below are almost identical and independent of the various locations unless stated accordingly.

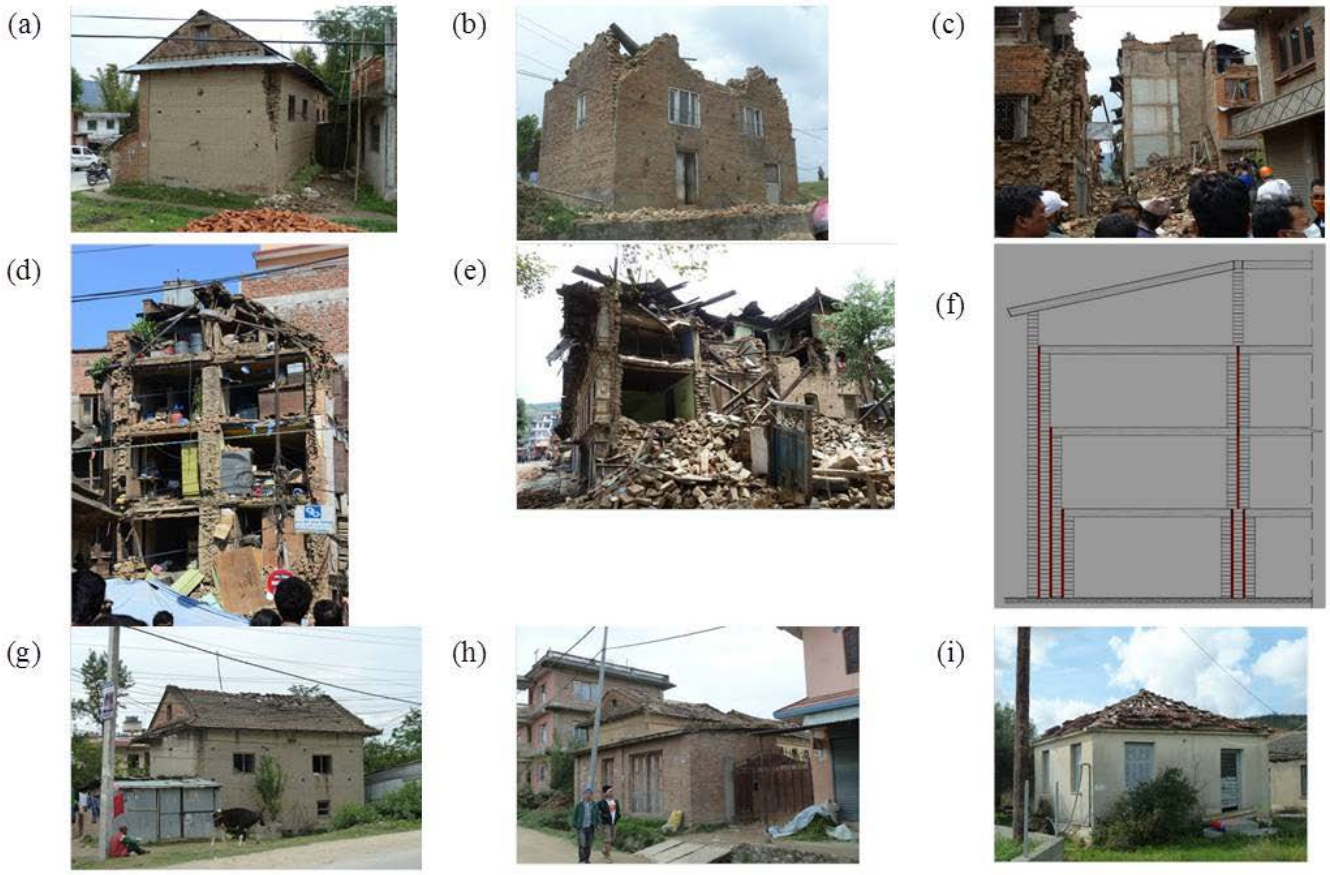

Fig. 3 – Representative seismic response of buildings during Gorkha earthquake. (a) The top parts of the four corners have symmetrically fallen vertically right down. (b) In addition to (a), the damage is initiated from the top-roof, the window glass panels are intact, the debris are spread symmetrically around the building. (c) Newer buildings use the walls of the adjacent order ones without any connection, and the respective walls of the newer buildings are free-standing vertical cantilevers. (d) Small or no movement of free standing objects as well as of the content of severely damaged buildings. (e), (f) The various vertical layers of the walls are independently built each other without any connection between themselves. (g) and (h) Roof tiles have been, symmetrically to the roof tree, dislocated similarly to Cephalonia, 2014 case, as shown in (i).

The response of monumental structures was very poor compared to the rather low recorded ground accelerations. It was observed that the structures were constructed out of solid fired clay bricks built either without mortar or with an earthen one. This mortar did not possess any bond with the bricks. The response of a great number of traditional structures was equally very poor although a considerable number of buildings of this category weathered the earthquake without any damage in spite of the fact that the quality of the workmanship was low. The height of these structures reaches the four and in some cases the five levels including the roof. Almost all the horizontal load bearing elements (roofs, floors and lintels) are from timber. In some cases the timber floors and lintels are strengthened with steel beams. The floor beams penetrating the walls are functioning as levers in the vertical plane against the stability of the above standing wall. This is especially pronounced during a vertical excitation of the floor.

In general, the walls have a thickness of 50 – 70 cm composed out of vertical layers of brick, but those multiple layers do not always possess a transverse connection between themselves, as it is shown in Fig.3a,b,e,f. In this way the masonry is quite vulnerable in horizontal and vertical ground excitations. In severely damaged buildings these independent and rather thin walls buckled vertically. The transversally connected walls have not any solid structural connection and the walls are freely standing. Any tie through the roof is ineffective. The cracks were limited in density, length, thickness and were mainly horizontal or vertical, and did not form the well knows X shape. In many cases it was evident that the damage was caused by the roof that vertically impacted the walls. Another worth mentioning characteristic of the response of this type of buildings is that it was not observed any horizontal relative motion or impact between adjacent buildings or any noticeable damage of the secondary elements, or motion of the free standing objects and, in general, content of the buildings, as it is shown in Fig. 3. In slightly or not damaged buildings the roof tiles were symmetrically dislocated starting from the roof tree. This mode of damage was also observed during the Cephalonia, 2014 earthquake as it is shown in Fig. 3g, h, i.

The symmetrical and around the vertical axis damage of masonry buildings with the top parts of the corners to be shacked off, forming a V shaped failure as it is shown in Fig. 3a and 3b, became a subject of a special investigation following a reverse analytical procedure. Namely, knowing the response of the structure we tried to define the excitation. The said shape of failure is observed not only in the numerous sites in Nepal after the recent event, but also in many other epicentral regions of destructive earthquakes in the past.

In order to investigate this mode/pattern of failure a simple masonry building 7.0 m x 7.0 m in plan, and 3.5 m height was selected as test model that was shaked with almost all probable types of ground excitations at a time (horizontal and vertical, natural and artificial earthquake time histories, half and full cycle pulses or harmonic type, combined with a variety of peak accelerations up to 1.5g). As a judging criterion for the most probable one or more ground excitation, was set the shape of the developed isostress lines, in the walls of the model after the pertiment analytical calculations, to be as close as possible to the observed in the field, the said V shaped failures. After numerous trials, the most probable excitation was proved to by that of a half cycle vertical pulse as a ground motion with an acceleration that exceeds 1.0g. The response of the model was almost not sensitive to a variety of the duration of the half cycle pulse of the vertical base excitations.

(a) (b) (c)

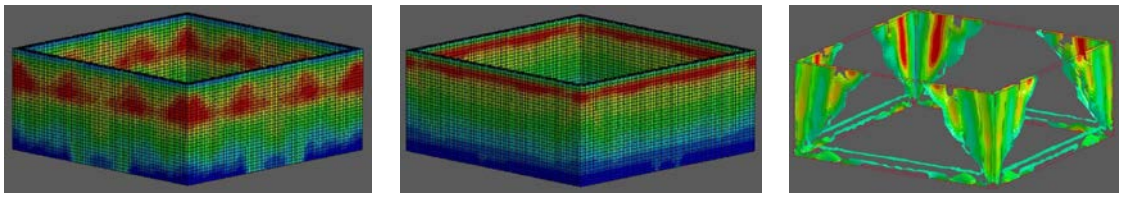

Fig. 4 – (a, b, c) A simple in plan of 7.0 m x 7.0 m and in height of 3.5 m masonry house without roof, under a vertical strong impact motion gave isostress lines identical to those observed at numerous sites (compare with damage pattern of Fig. 3 a,b).

Contemporary buildings can be divided in two groups. The first includes buildings built before 1996, when the first building code of Nepal was put in force. The height of these buildings is less than 7 – 8 stories. In general, their load bearing system is reinforced concrete filled with solid fired clay brick walls. The dimensions of the concrete elements are very small, remaining constant along the height of the building. For example, the central columns of a 5-6 storied building are 0.25 m x 0.25 m ÷ 0.30 m x 0.30 m at distances of 4 – 5 m. In general, the quality of concrete and workmanship is poor. The reinforcement is sparse and small in diameter. Shear walls were not used. Their flexibility is augmented due to soft soil conditions, small plan dimensions and many stories.

Fig. 5 – Representative seismic response of buildings during the Gorkha earthquake. (a) Contemporary buildings having a smashed ground or intermediate floor. (b) The location of the damage may occur at any point along the height of the structure, depending on the point of interference of incident and reflected vertically propagated seismic waves. (c), (d), (e) and (g) it was observed no relative motion between adjacent buildings of any type at different sites. (f) A close-up of the adjacent top part of the buildings shown in the picture (e). (h) and (i) Two flexible contemporary adjacent 8 storied buildings possess at their top a common and untied point, which has not been cracked, unlike the quite commonly anticipated impact, or at least, detachment after earthquakes.

As it is shown in Fig. 5 two types of response of these buildings are clearly distinguished: In the first type (Fig.5d, e, g, h), which covers the majority of the buildings, there was no damage, the glass panels were intact and not horizontal motion or impact was detected. This observation is quite interesting since, in spite of the quite unfavorable combination of a high magnitude earthquake at distances of the order of 30 – 80 km, on rather deep soft soil conditions and flexible multistoried buildings, the resulting building horizontal motions were null. The same is observed in the category of traditional and stiffer structures. In the second type, which covers a very small number of buildings, there was total or partial collapse. The collapse was within the plan of the building in a pan-cake mode (Fig. 5a). The failure mode, could be found at three distinguished locations as it is schematically shown in Fig. 5b: At the ground floor, at any intermediate level, or at the top level. The same mode of failure was also observed in the previous category of traditional buildings.

Buildings constructed after 1996, following the national earthquake code are much safer. Those buildings have a height of up to 20 stories, are more stiff and of sounder design and construction quality. Nevertheless, it was not possible to exclude this category of buildings to have suffered the type of damage shown in Fig. 5a.

During the visit, the team investigated several infrastructure works as for example a rather long span, suspended, bridge, an arched bridge, several other smaller bridges and retaining walls, along the road, and observed no damage, displacement or dislocation except the pedestrian bridge and relevant infrastructures that were adjacent to the emerging fault as already exposed in previous section.

4. CHARACTERISTICS OF THE KANTI PATH RECORD OF THE NEPAL-GORKHA EARTHQUAKE

Near-fault ground motions are affected by directivity phenomena, which produce important velocity pulses, mostly associated with the normal to the fault direction. Directivity pulses amplify the long period coherent component of the ground motions and are explicitly apparent in the velocity and the displacement time histories and the related response spectra. A number of methods are commonly used for the identification of the parameters of the velocity pulses, mainly their period and amplitude. Also, several mathematical expressions have been proposed for their mathematical representation, which vary from simple functions to more complicated wavelets. A very efficient wavelet is the one proposed by Mavroeidis and Papageorgiou (M&P) [10], which, beyond the period and the amplitude, uses additional parameters related to the total duration and the phase shift of the pulse. In this paper, a recently proposed new method [11] is used, which allows the explicit determination of the parameters of the pulse contained in pulse-like records. The M&P wavelet is used for the mathematical representation of the pulse. First, the period of the pulse is determined from the peak of the $S_d \times S_v$ *product spectrum*, a new concept defined as the product of the velocity and the displacement response spectra. The remaining parameters of the M&P wavelets are derived from the targeted response spectrum of the ground motion using an iterative procedure and defining subsequent wavelets from the residual ground motion after each iterative cycle. The method follows a well-defined procedure easily implemented in a computer code for the automatic determination of the pulse parameters of a given ground motion. The proposed method can be extended to the determination of additional pulses inherent in the ground motion. To this end, the detected significant pulse is subtracted from the original record to derive the *residual record*, to which the method is applied for the derivation of the second pulse. This procedure can be repeated several times until all significant pulses are derived. The summation of all significant pulses produces a very accurate mathematical representation of the original record.

In the case of the Kanti Path record a sequence of six pulses has been determined in order to define the velocity time history and the relevant spectra. As seen in Fig. 6a, the approximation of the velocity time history with the six pulses is almost perfect. The same is observed for the relevant velocity spectra (Fig. 6b). The main characteristic of the record are its low acceleration values, close to 0.15g as can be seen in Fig. 7a, b which may be due to the soil deposit filtering at the recording site, where the V_s30 is approximately 200 m/sec [8]. The other characteristic of the strong ground motion is the directivity effect, pronounced in the two horizontal components, where strong velocity pulses with period around 5.0 sec and amplitude of approximately 80 to 100 cm/sec are observed (Fig.7a, b). In what regards the acceleration spectra, a bell-shaped amplification is observed (Fig.7c, d), in agreement with [9], around the pulse period, which is also the predominant period of the acceleration spectrum for the east component of the record.

a)

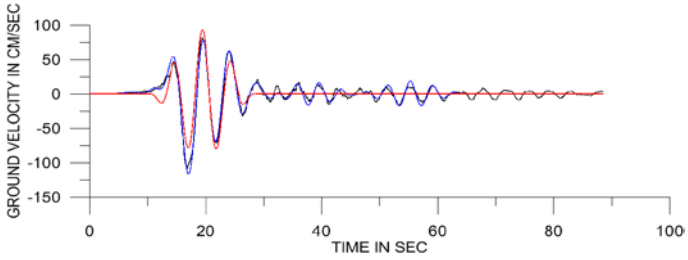

b)

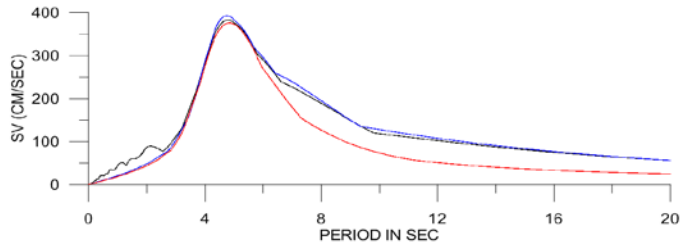

c)

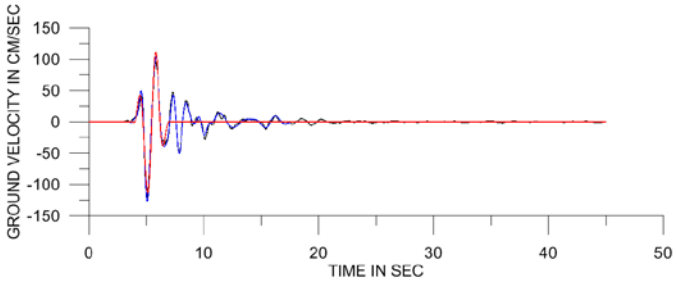

d)

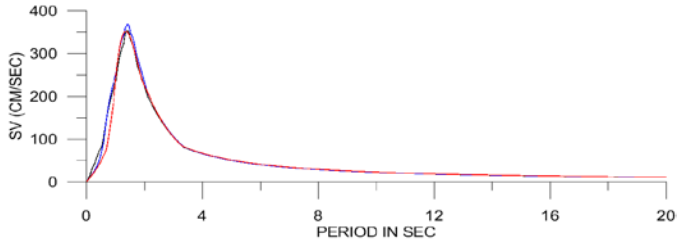

Fig. 6 – In the above figure a) the velocity time history of the eastern component of the Kanti Path record is presented, where the original time history is given in black, the combination of six pulses in blue and the first dominant pulse in red. In b) the relevant velocity spectra are given with the same colour identification. In c) and d) the velocity time history and velocity spectra are given for the Lixouri eastern component of the Cephalonia 2014 earthquake.

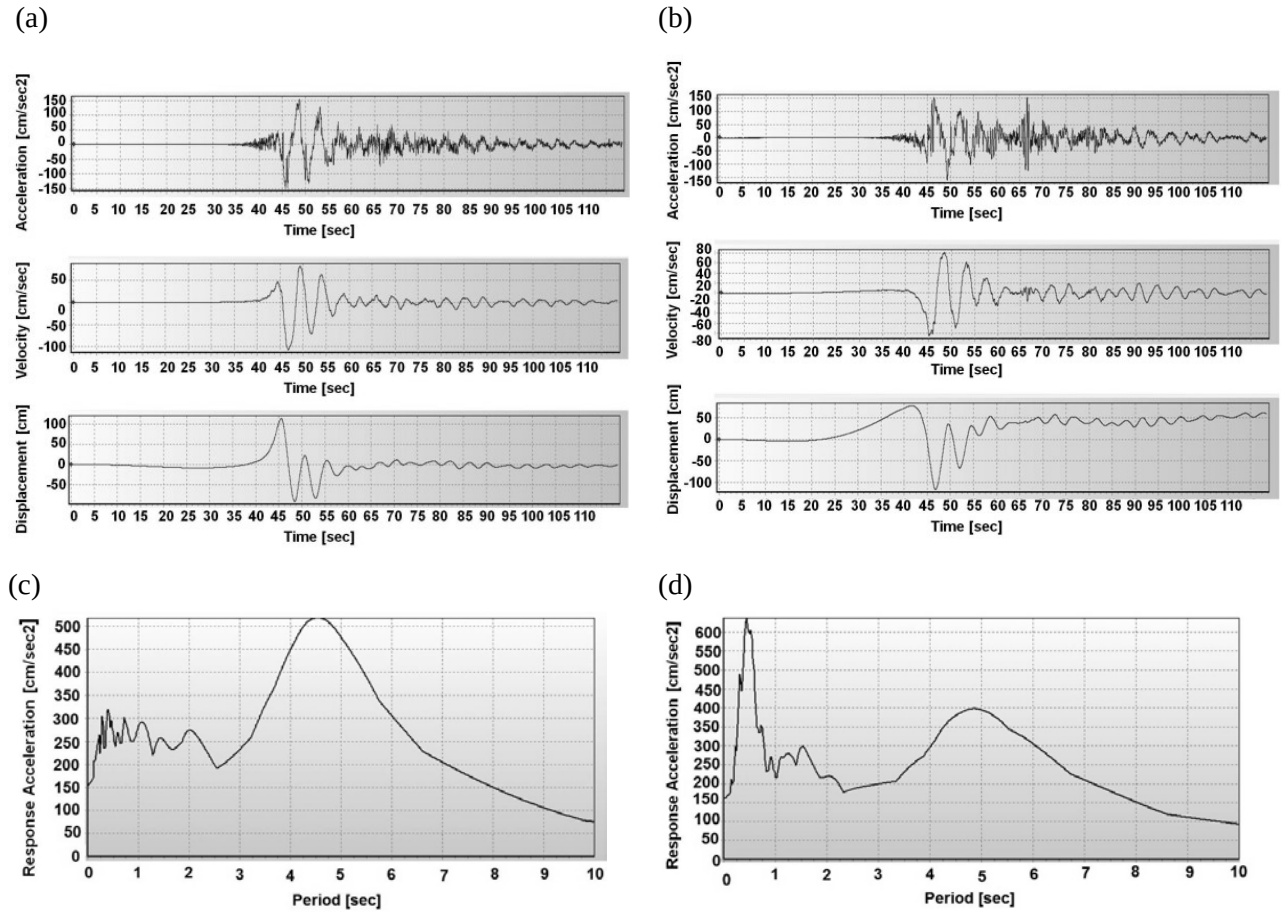

Fig. 7 – Ground motion time histories for Kanti Path record a) East component b) North component. c), d) Relative acceleration spectra.

The velocity spectra of both Kanti Path components present a predominant period around 5.0 sec, which is close to the pulse period. An analysis performed according to the method of [11], in order to evaluate the M&P [10] wavelets that can mathematically simulate the velocity time history, showed that the east component of the record includes an M&P wavelet with a period of 4.99 sec, amplitude of 93.21 cm/sec and a large number of pulse cycles. The cross correlation coefficient between the original velocity time history and the extracted wavelet is 90% presenting a very good fitting. The north component includes a wavelet with a period of 5.39 sec and amplitude of 87.87 cm/sec. The cross correlation between the original velocity time history and the extracted wavelet is 83%. The two horizontal velocity time histories are closely correlated with a coefficient of 76%. The period of the directivity pulses is, as well known, exponentially related to the event moment magnitude and in this case close to the predicted values.

The maximum ground velocity values for the two horizontal components are about two thirds of the mean value of the expected fault slip velocity which is about 150 cm/sec and are a good estimate for directivity pulse amplitudes near large ruptured asperities. A case with similar ground velocity, filtered high frequency non-coherent component of the ground motion due to the soil deposit, and a pulse period quite smaller and equal to 1.49 sec, was observed during the Cephalonia earthquake of 2014 [12]. In this case the correlation coefficient between the first dominant pulse and the original record was 88%, an also very good fitting. At the recording site the V_s30 is approximately 270 m/sec. As it is observed from these two records, the pulse period is a function of the moment magnitude of each event but the maximum ground and spectral velocities are similar, close to the maximum, up to now, observed values and not affected from the event magnitude. These observations are consistent with those referred in [10].

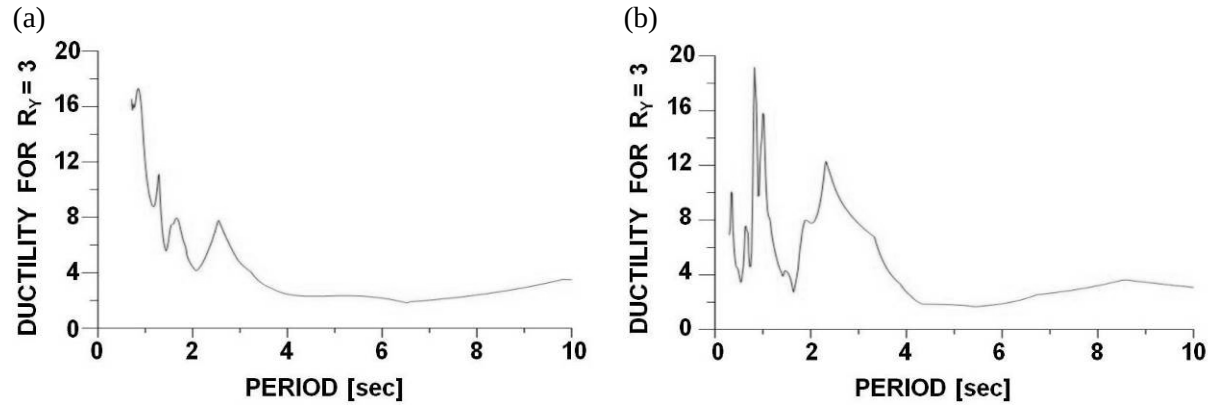

Fig. 8 – Ductility for Ry=3 in a) and b) for the east and north ground motion components.

What is interesting in both cases is that the non-coherent high frequency component of the ground motion is almost absent (possibly due to soil filtering) and the coherent low frequency part is dominated by the directivity pulse, which is predominant even in the acceleration time history. In both cases the acceleration of the extracted wavelet is equal to the acceleration of the original record (0.15g for Gorkha and 0.6g for Cephalonia) if we consider that the maximum pulse acceleration is equal to the product of the maximum pulse velocity with the circular pulse frequency. As a result the peak spectral accelerations are estimated at the pulse period and the shape of the acceleration spectrum is different from the usual one taken into account in the regulations.

Furthermore, the ductility demand was calculated for R_y=3. Here again the effect of the directivity is also evident. In agreement with the observation made in [13], the ductility values are quite larger than the reduction factor at a period range lower than half the pulse period see Fig. 8a, b.

5. CONCLUSIONS

The earthquake of the April 25th event caused a wide ground deformation zone associated with thrust faulting and mainly the formation of monocline–like escarpments associated with open tension cracks and small-amplitude folds, confirming the early models of co-seismic slip which suggest that the largest amount of slip on the fault was located just below the city of Kathmandu.

The earthquake intensity in the broader epicentral area was comparatively low. Monumental and traditional buildings suffered the majority of damage due to inadequate construction and maintenance. In case of sounder construction, buildings remained intact.

The majority of the contemporary buildings with a reinforced concrete load bearing system and brick wall partitions, in spite of the fact that in the majority of the cases possessed high seismic vulnerability, weathered the earthquake without damage. Other structures as bridges, retaining walls etc. did not present noticeable damage.

All over the examined and quite extended region, numerous cases were reported in which not any relative lateral motion between adjacent buildings of any kind was observed. There was also observed either partial or total collapse of buildings or no horizontal motion, no cracks, no braking of glass window panels. In all cases we did not observe X shaped cracks. This fact is a key characteristic of dominance of vertical excitation and respective response of structures, a fact characterizing the epicentral region. In other words, epicentral region's characteristics were unusually quite extended in this event.

In agreement with the said findings, following a reverse analytical procedure we defined a type of ground motion compatible with the observed pattern of structural response. This type of ground motion contains a half cycle vertical pulse with a peak acceleration exceeding 1.0g.

The Kanti-Path record presents a coherent low frequency content dominated by directivity with an insignificant non-coherent high frequency component. This phenomenon appears characteristic if there is a

combination of soft soil deposits with directivity affected ground motion, near large slip areas, as in a smaller event in Cephalonia, Greece, 2014. The difference in pulse period for each case is due to the event magnitude and is related to the relevant rise time and radius of the ruptured asperities. A further characteristic of both records is the similar ground velocity amplitude close to the mean value of the slip velocity, considered about 150 cm/sec. It is possible that such values are representative of an upper level of directivity affected peak ground velocities, close to large asperities, independent of the moment magnitude.

The authors consider that there are still items that deserve time and research efforts to be clarified and widely accepted.

7. REFERENCES

[1] Bilham R (2004): Earthquakes in India and the Himalaya: tectonics, geodesy and history, *Annals of Geophysics* **47** 839-858.

[2] Bilham R (2009). The seismic future of cities, *Bulletin of Earthquake Engineering*, **7**, 839-887.

[3] Bilham R, Gaur VK, Molnar P (2001): Himalayan seismic hazard, *Science*, **293**, 1442–1444.

[4] Hodges, K.V. (2000). Tectonics of the Himalaya and southern Tibet from two perspectives, *Bulletin of the Geological Society of America*, **112**, 324-350.

[5] Avouac J-P, Ayoub F, Leprince S, Konca O, van Helmberger D (2006): The 2005, Mw 7.6 Kashmir earthquake: Sub-pixel correlation of ASTER images and seismic waveforms analysis. *Earth and Planetary Science Letters*, **249**, 514-528.

[6] Chamlagain D, Gautam D (2015): Seismic hazard in the Himalayan intermontane basins: an example from Kathmandu Valley, Nepal. In: Shaw R, Nibanupudi HK (eds) Mountain hazards and disaster risk reduction. Springer, Japan, pp. 73-103.

[7] USGS United States Geological Survey (2015): M7.8 - 34 km ESE of Lamjung, Nepal. http://earthquake.usgs.gov/earthquakes/eventpage/us20002926

[8] Paudyal YR, Yatabe R, Bhandary NP, Dahal RK (2012): A study of local amplification effect of soil layers on ground motion in the Kathmandu Valley using microtremor analysis. *Earthquake Engineering and Engineering Vibration*, **11**, 257-268.

[9] Shahi SK, Baker JW (2011): An empirically calibrated framework for including the effects of near-fault directivity in probabilistic seismic hazard analysis. *Bulletin of the Seismological Society of America*, **101**, 742-755.

[10] Mavroeides GP, Papageorgiou AS (2003): A mathematical representation of near-fault ground motions. *Bulletin of the Seismological Society of America*, **93**, 1099-1131.

[11] Mimoglou PP, Psycharis IN, Taflampas IM (2014): Explicit determination of the pulse inherent in pulse-like ground motions. *Earthquake Engineering and Structural Dynamics*, **43**, 2261-2281.

[12] GEER Association Report (2014). 2014 Cephalonia, Greece Earthquakes. Report No. GEER-034

[13] Iervolino I, Cornell CA (2008): Probability of occurrence of velocity pulses in near-source ground motions. *Bulletin of the Seismological Society of America*, **98**, 2262-2277.